

# EOC Project Final Report

## **Operational AVHRR processing modules: atmospheric correction, cloud masking and BRDF compensation**

A. C. Dilley, M. Edwards, D. M. O'Brien and R. M. Mitchell.  
CSIRO Atmospheric Research  
Private Mail Bag 1  
Aspendale Victoria 3195  
Australia

May 2000

# 1 Introduction

This is the final report on the EOC project “Operational AVHRR processing modules: atmospheric correction, cloud masking and BRDF compensation”. AVHRR is an acronym for Advanced Very High Resolution Radiometer, a scanning radiometer flown on the Advanced Tiros-N (ATN) series of satellites. BRDF is an acronym for Bi-directional Reflectance Distribution Function.

The objectives of this project are to provide operational software and data for the following tasks:

- (i) maintenance and upgrading of the CalWatch data base;
- (ii) automatic cloud masking, with thresholds set according to location and season;
- (iii) correction of reflectances for atmospheric scattering and absorption using analysed meteorological fields for water vapour and either observed or climatological estimates of aerosol;
- (iv) correction of AVHRR to standard illumination and observation geometry using BRDF models determined as part of a separate EOC task.

All objectives of the project have been achieved: the CalWatch data base has been extended and modified to improve accessibility and modules CloudMask, reflectance, AtmosphericCorrection and BRDFCorrection have been written and implemented to provide cloud detection and atmospheric and BRDF correction of remotely sensed radiances.

Modules developed under the terms of the present project are supplied in a package that contains all the code and data necessary for complete processing of raw AVHRR data through to an output product comprising calibrated, navigated, cloud-flagged, atmospherically and BRDF corrected reflectances. The package, known as Modular AVHRR Processing Software (MAPS), also contains test data and programs that can be used to check correct installation as well as demonstration data and programs that can be used to reproduce the images included in this report. The MAPS modules are shown in relation to each other, the CalWatch data base, available data sets and supplementary programs in figure 1. The MAPS package comprises all modules and data drawn beneath the DISIMP image data box (with the exception of the CalWatch data which may be obtained independently via FTP). The ASDA to DISIMP converter and SATLOC programs can also be provided but are not part of the MAPS package

All modules are written in Fortran 95 and make full use of that language’s clarity, elegance and emphasis on modular construction. Modules are self-documenting and make reference to relevant source material where appropriate. Details of modules and programs are given in the sections that follow.

Examples of images generated by MAPS are shown in figures 2 and 3. The images shown there are based on data recorded on two successive orbits and hence under two significantly different illumination and observation geometries. The upper image of figure 2 shows uncorrected top of the atmosphere reflectances (reflectance factor divided by the cosine of the sun zenith angle) for band 2. A marked discontinuity in reflectance can be seen along the join-line of the two images, here set at the mid-point of the overlap region. The lower image of figure 2 shows the same data corrected for atmospheric effects using a modified form of the model proposed by Mitchell and O’Brien (1993) and corrected to a standard illumination and observation geometry using POLDER data and the BRDF model of Roujean et al. (1992). Elimination of the discontinuity in reflectance between data derived from the two orbits illustrates the effectiveness of these models and the code that implements them.

The upper image of figure 3 shows the original data corrected for atmospheric effects alone while the lower image shows corrections to a standard geometry alone. The series of images shown in figures 2 and 3 suggests BRDF corrections dominate the correction process. It should be noted, however, that atmospheric corrections introduce a significant shift in reflectance values that differs in magnitude between spectral bands and hence generates significant shifts in Normalised Difference Vegetation Index (NDVI) values (defined as  $(R_2 - R_1)/(R_2 + R_1)$  where  $R_1$  and  $R_2$  are reflectances based on bands 1 and 2 respectively).

The effect of corrections on NDVI values is illustrated in figure 4. The top image shows a cloud- and sea-masked image of NDVI based on uncorrected top of the atmosphere reflectances. The bottom image shows a similarly masked and identically scaled image of NDVI based on reflectances corrected for atmospheric effects and corrected to a standard illumination and observation geometry using the

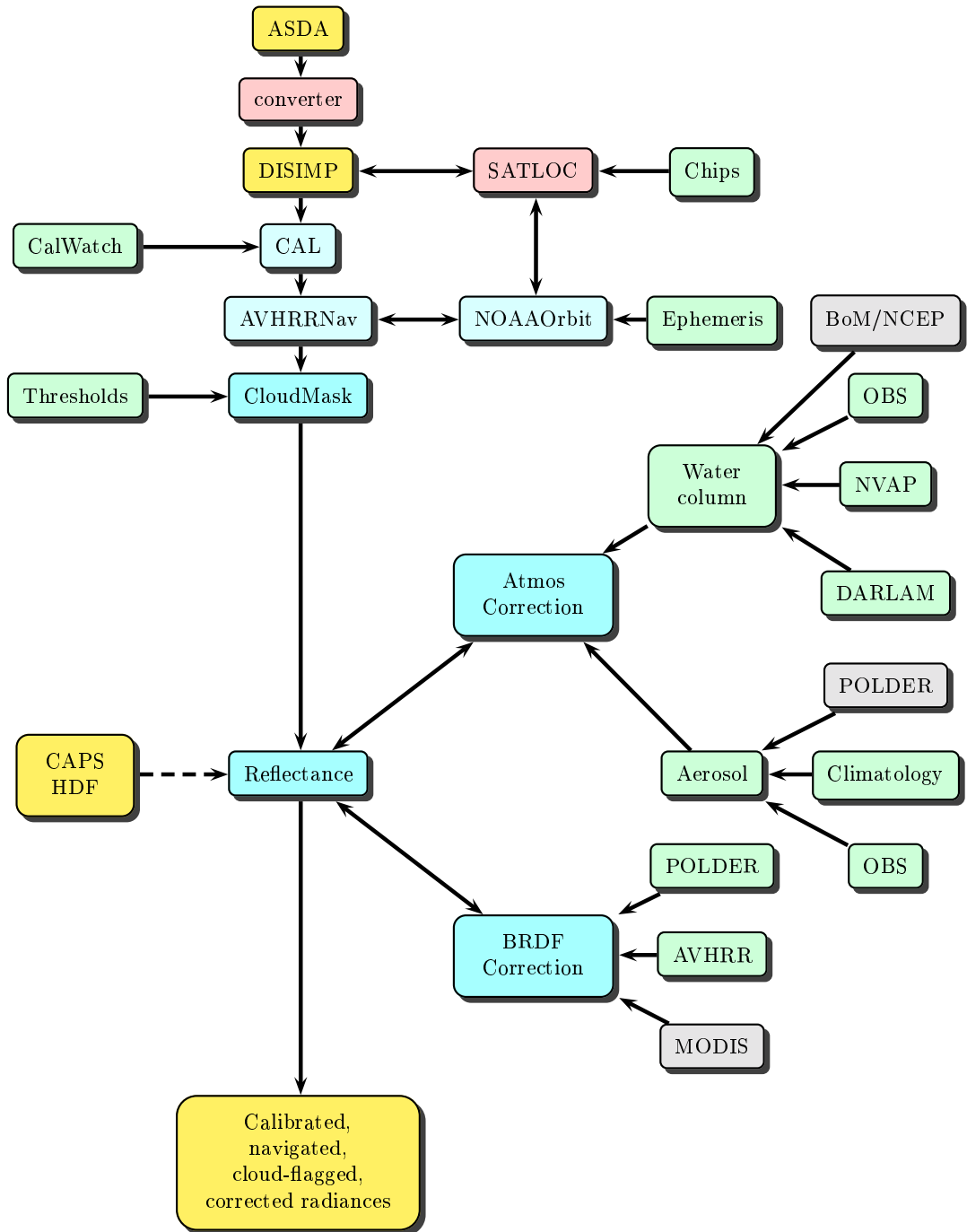


Figure 1: MAPS modules and other related software and data: blue — modules; red — stand-alone programs; yellow — image data; green — other data; grey — possible future data sources. The darker blue indicates modules developed as part of the present EOC project. The dashed arrow indicates a planned but as yet unbuilt connection.

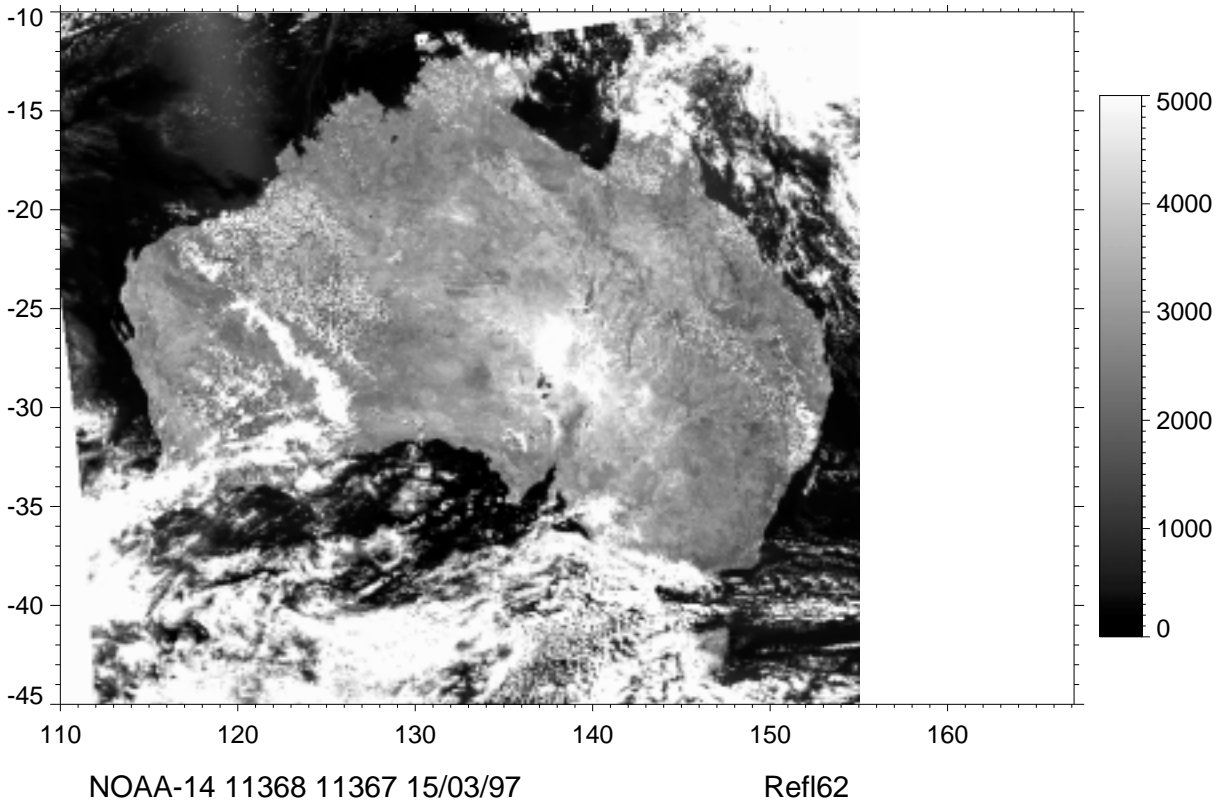
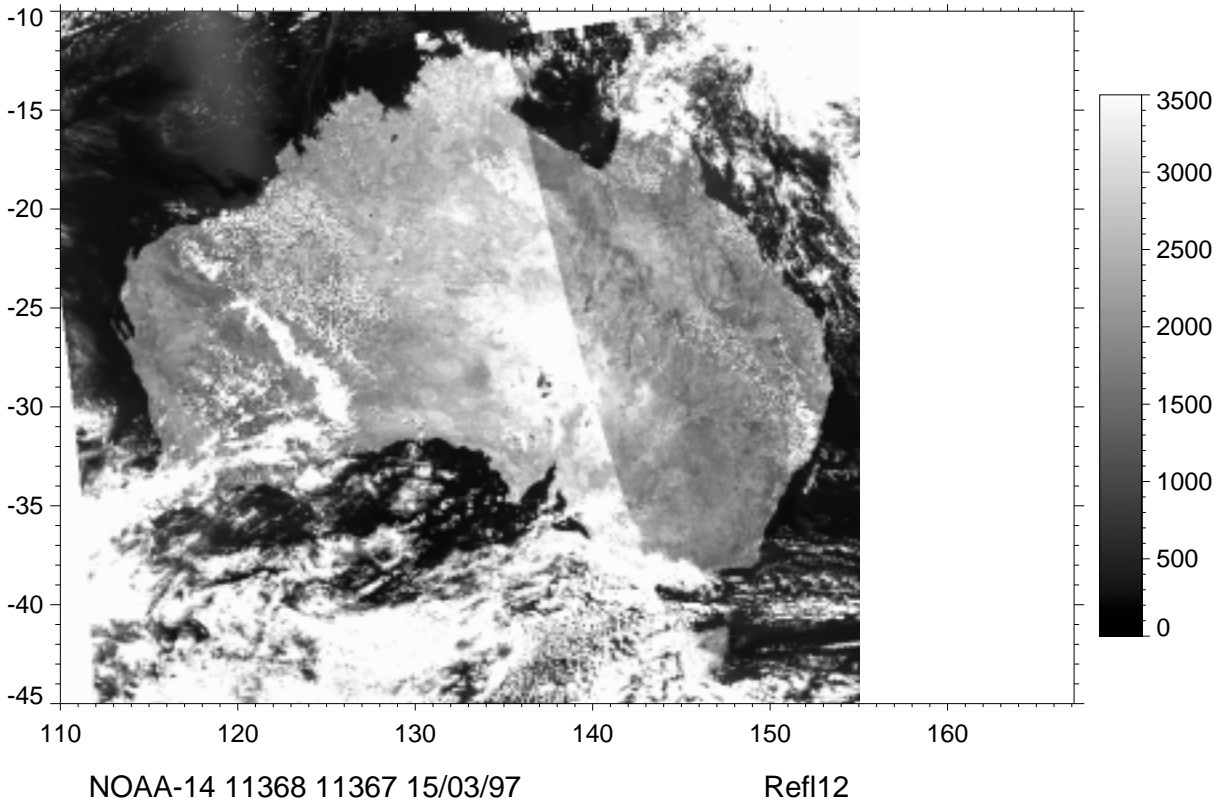


Figure 2: Above: an AVHRR composite image of Australia based on data from two successive orbits processed to yield uncorrected, band 2 reflectances at the top of the atmosphere. Below: as above but with data processed to give surface reflectances corrected to a standard illumination and observation geometry.

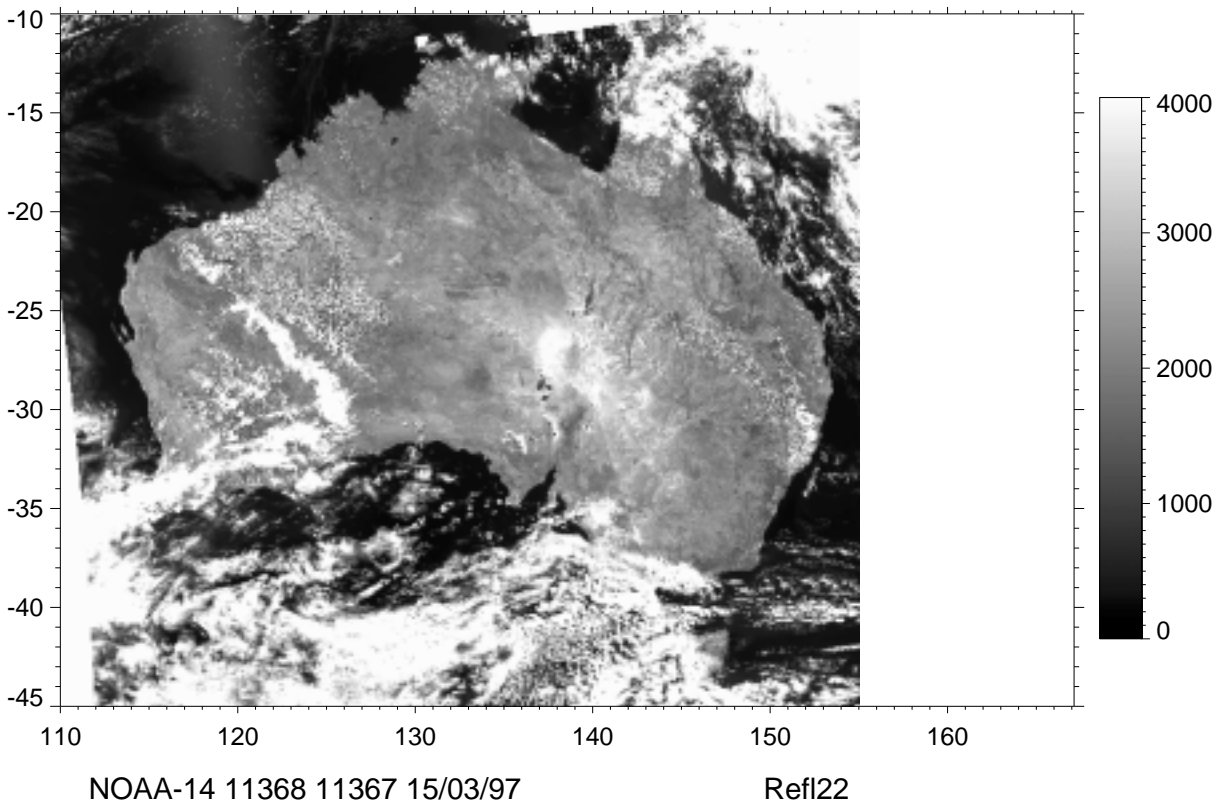
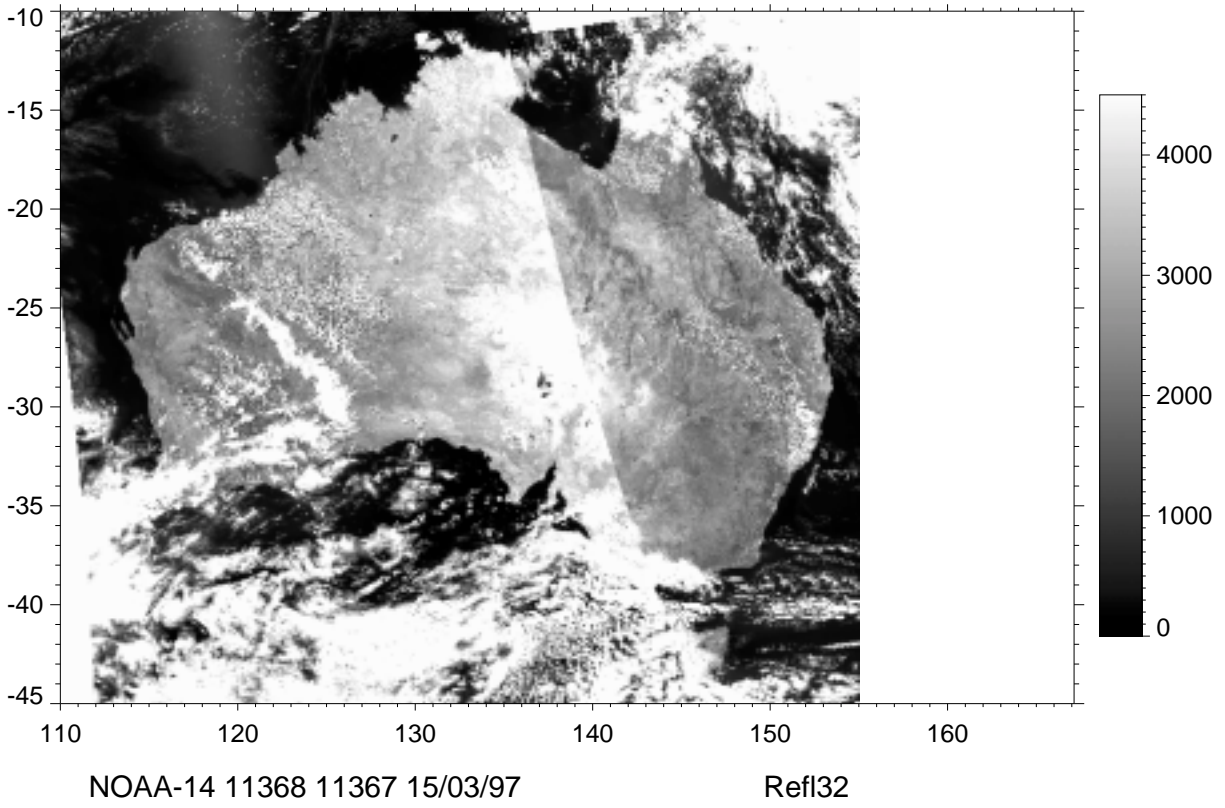


Figure 3: Above: an AVHRR composite image of Australia based on the same data as figure 2 but with data processed to give atmospheric correction alone. Below: as above but with data processed to give reflectances at the top of the atmosphere corrected to a standard illumination and observation geometry.

procedures outlined above. The middle image is similar to the top image but is scaled to make its colour range comparable with the bottom image. The discontinuity in NDVI apparent in the top image, and more evident in the middle image, is eliminated in the bottom image where corrections have been applied.

Some further indication of the effects of the corrections employed here on reflectance and NDVI values is illustrated in figure 7 where uncorrected and variously corrected reflectances for nine sites in Victoria have been plotted. The data used in the generation of this figure and their relevance are discussed in greater detail in Section 4.5

The new modules are written to provide processing at the pixel level and therefore operate independently of data format and other data management software. This means that, while the test and demonstration programs used to produce the images of figures 2 and 3 (and supplied with the MAPS package) require input image data in DISIMP<sup>1</sup> format (and generate output image data in the same format), the modules work perfectly well with other data formats. Thus, for example, a link could be made to the CAPS package (Turner et al., 1998) using routines that read a CAPS-generated HDF<sup>2</sup> file. This file would need to hold all relevant data, namely, date and time of overpass and image data containing reflectance factors for the visible and near infra-red bands, sun illumination and satellite viewing angles and geographic locations. Such a link to CAPS is shown diagrammatically in figure 1. Code to make the connection has been planned but awaits funding to implement.

## 2 CalWatch

The CalWatch program (Mitchell, 1997) has for some time provided information via the World Wide Web on AVHRR solar band calibration coefficients and associated filter function parameters. The program draws on many earlier studies including those of Mitchell et al. (1992), Rao and Chen (1995), Mitchell et al. (1996) and Rao and Chen (1996).

Under the present project, CalWatch has been

- extended to cover satellites not previously covered (ie NOAA-7, -9 and -11),
- upgraded to provide the best available time-series of data covering all satellites from NOAA-7 through -15;
- re-organized to facilitate accessibility of data to software.

In addition, documentation for CalWatch has been extended and upgraded to facilitate accurate application of supplied data within the user community (Mitchell, 1999). As previously, the CalWatch document is accessible via the CSIRO Atmospheric Research (CAR) web site and is linked to the Earth Observation Centre (EOC) web site. The calibration data tables are accessible directly through the CAR FTP server.

## 3 Automatic cloud masking

For the past two years, a simple threshold-based algorithm has been used to mask cloud in the Grassland Curing Index (GCI) maps of Victoria automatically generated at CAR and supplied operationally to the Country Fire Authority (CFA) and power distribution companies (Dilley and Edwards, 1998a,b). The algorithm performs satisfactorily in the context of the GCI application for which it was developed. It could prove a useful initial benchmark against which other algorithms are tested.

The algorithm uses the AVHRR parameters of band 1 reflectance factor, spatial variance of band 1 reflectance factor, a simple function of the ratio of band 1 to band 2 reflectance factor and brightness temperature derived from band 4. For every element in an image, the value of each parameter is compared in turn with three pre-set threshold values for that parameter. Passing the first threshold test scores a point in favour of cloud, passing the second threshold test earns a bonus point (cloud very likely) and passing the third threshold test earns a demerit point (cloud very unlikely). After all four parameters are tested, the cloud mask is set if the point score totals 2 or more.

---

<sup>1</sup>Device Independent Software for Image Processing developed originally in the former CSIRO Division of Computing Research and subsequently at CSIRO Atmospheric Research.

<sup>2</sup>Hierarchical Data Format

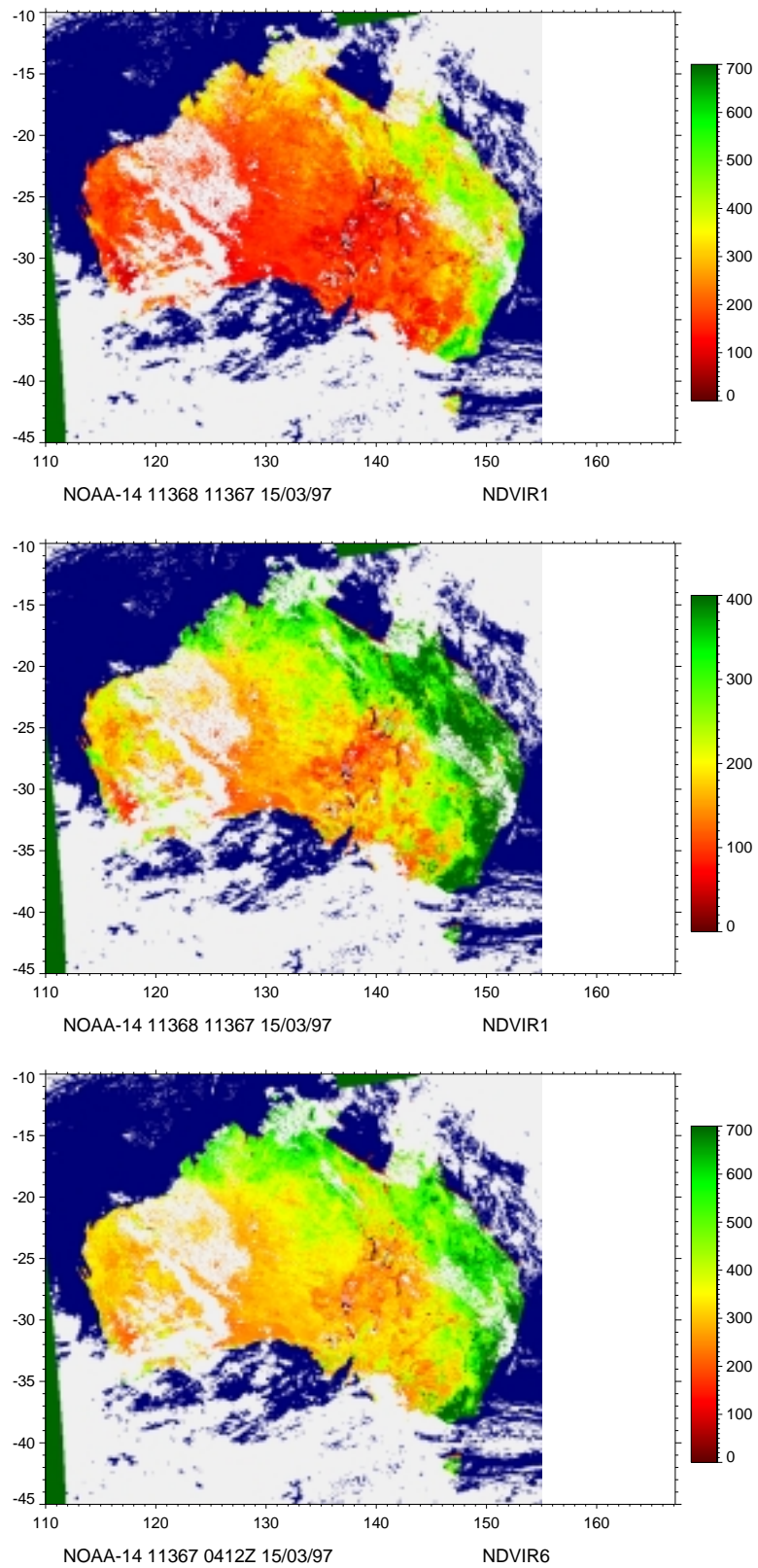


Figure 4: Top: an AVHRR composite image of Australia showing NDVI values derived using uncorrected, top of the atmosphere reflectances. The image is scaled to the same values as the bottom image. Middle: as for the the top image but scaled to values that facilitate comparison with the bottom image. Bottom: as for the above images but showing NDVI values derived using reflectances corrected for atmospheric effects and corrected to a standard illumination and observation geometry.

In the context of the GCI application, it is better for the algorithm to be biased towards overspecification of cloud rather than underspecification. Hence, cloud boundary problems are addressed using the simple expedient of extending the cloud mask by one or two image elements in all directions. Obvious improvements here would be to make the direction of extension dependent on sun azimuth and the extent dependent on cloud height.

### 3.1 Module CloudMask

Under the present project, the cloud mask algorithm currently used for GCI analysis has been re-coded as a module named CloudMask. The module is configured to use sets of threshold values differentiated by month of year.

CloudMask has been tested thoroughly only in relation to the application for which it was developed — namely in the production of GCI maps. While some further testing outside these constraints is planned, it is hoped that others may use the module to explore its performance in a wide range of conditions.

### 3.2 Demonstration code and data

Module CloudMask is supplied as a product of the present project.

In addition we make available a demonstration program named Cloud2000 that takes raw AVHRR data written in DISIMP format and generates six output channels as follows:

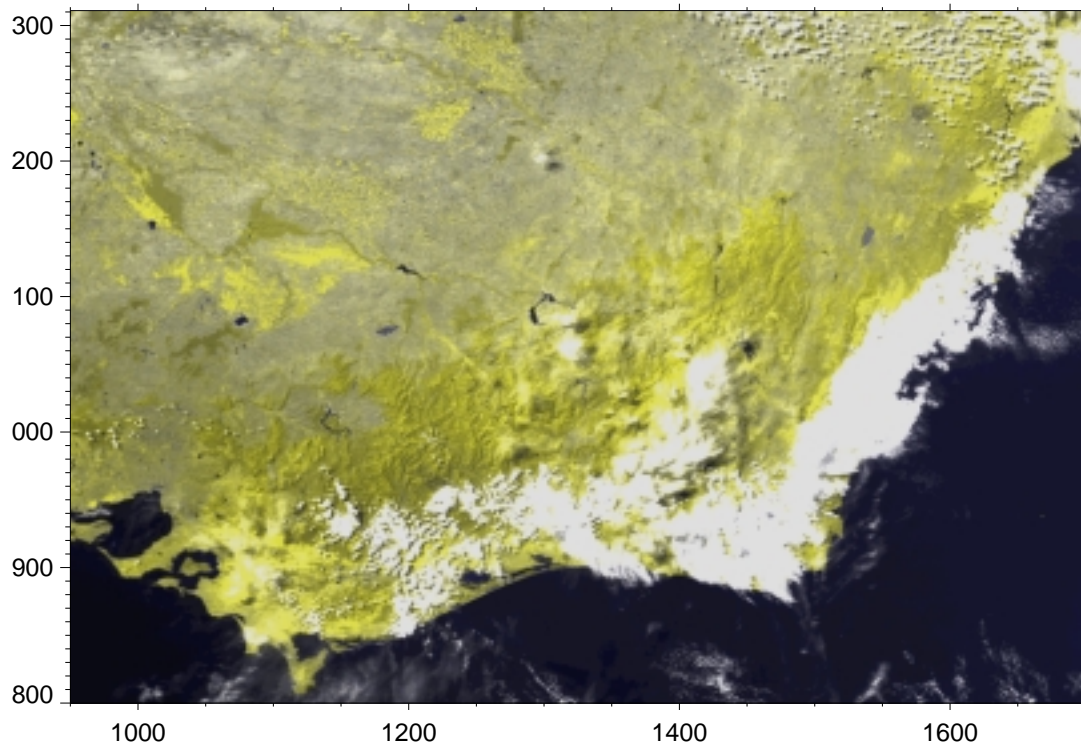
- channel 1 reflectance factor for band 1 \* 100 (ReffF1)
- channel 2 reflectance factor for band 2 \* 100 (ReffF2)
- channel 3 brightness temperature for band 4 \* 100 (BTemp4)
- channel 4 variance of reflectance factor for band 1 \* 100 (VarnR1)
- channel 5  $ABS(A - (ReffF1) / (ReffF2)) * 100$  where A is a constant (RaR1R2)
- channel 6 cloud mask ( 0, 1 ) (CldMsk)

Here reflectance factor is generated using the module shown as ‘CAL’ in Fig 1. In reality, ‘CAL’ is a generic name encompassing two modules, AVHRRVisCal and AVHRRThmCal. AVHRRVisCal accesses the CalWatch data base to retrieve appropriate coefficients and then converts the raw data of AVHRR bands 1 and 2 (and 3a for NOAA-15) to any one of reflectance factor or in-band radiance or mean spectral radiance. Brightness temperature is generated using AVHRRThmCal. This module accesses calibration coefficients derived from on-board measurements located in the DISIMP file and then converts the raw AVHRR thermal data counts to either in-band radiance or brightness temperature. Both modules use look-up tables to enhance speed of computation.

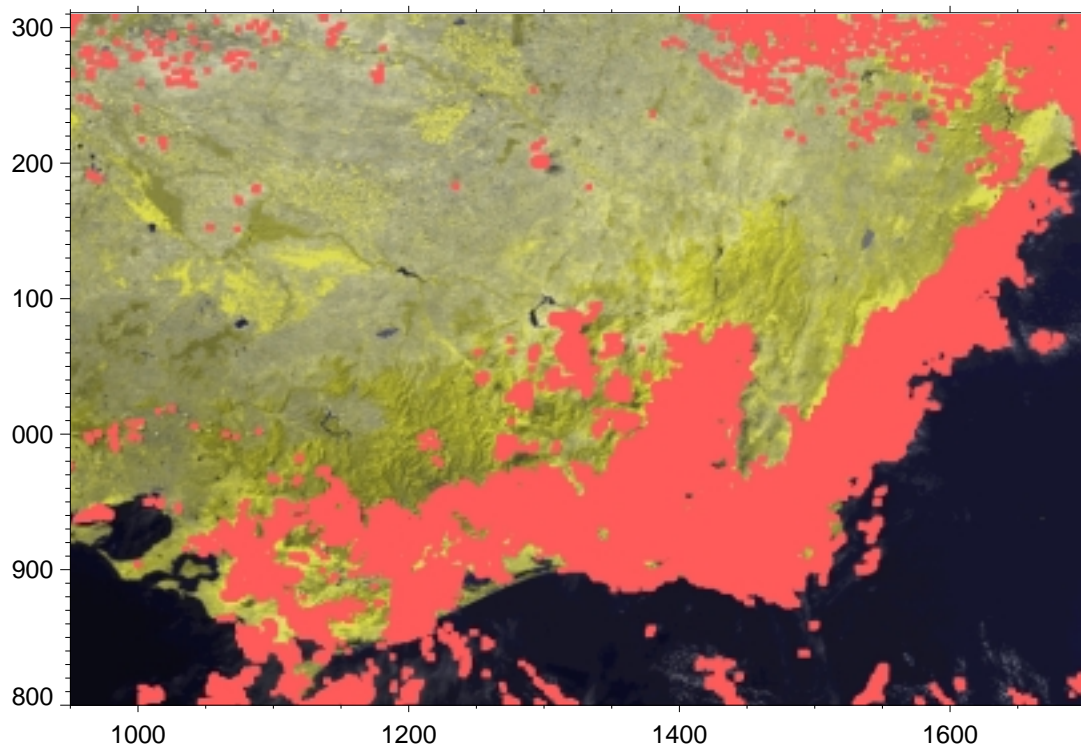
Cloud2000 was used to generate the images of figure 5. The cloud mask shown there represents the case where one wishes to reduce the risk of cloud contamination in unmasked areas. Thresholds were biased towards cloud detection and the cloud expansion was set at two image elements. More conservative thresholds could be set and the cloud expansion could be reduced to one image element or removed altogether with commensurate reduction in masked area. All data files and modules required to reproduce these images have been included in the MAPS package.

## 4 Atmospheric and BRDF correction

Because radiance reflected to space depends upon both the reflectance of the surface and the scattering and absorption properties of the atmosphere, the two processes must be considered simultaneously in correcting AVHRR shortwave bands for the effects of BRDF and atmosphere. The coupling between the processes was taken into account by Mitchell and O’Brien (1993), who showed how AVHRR data may be corrected accurately and efficiently if both the functional form of the indicatrix, defined to be the BRDF normalized by the surface albedo, and the optical properties of the atmosphere are known from independent data. The software described in this report follows the approach advocated by Mitchell and O’Brien (1993). The indicatrix is taken from independent satellite data (such as POLDER), the water vapour field is derived from a meteorological forecast model (DARLAM), and the aerosol properties are obtained from either climatology or observations, if the latter are available. The software produces a variety of products, including the surface albedo and the surface reflectance with the sun and observer located at standard positions.



Noaa-14 21527 0549z 05/03/1999



Noaa-14 21527 0549z 05/03/1999

Figure 5: Above: realistically coloured, two-band image of eastern Victoria. Below: the same image as above overlaid with cloud mask generated by program Cloud2000. Cloud expansion is set at two image elements.

Number	Algorithm	Indicatrix	Product	Remapping	Symbol
1	UNIT	$g = 1$	Reflectance	None	$R_d(\theta_0, \phi_0, \theta, \phi)$
2	UNIT	$g \neq 1$	Reflectance	Sun & sat	$\hat{R}_d(\overline{\theta_0}, \overline{\phi_0}, \overline{\theta}, \overline{\phi})$
3	ATCO	$g = 1$	Albedo	None	$\hat{\alpha}_d(\theta_0)$
4	ATCO	$g \neq 1$	Albedo	None	$\hat{\alpha}_d(\theta_0)$
5	ATCO	$g \neq 1$	Albedo	Sun	$\hat{\alpha}_d(\overline{\theta_0})$
6	ATCO	$g \neq 1$	Reflectance	Sun & sat	$\hat{r}_d(\overline{\theta_0}, \overline{\phi_0}, \overline{\theta}, \overline{\phi})$

Table 1: List of products from the atmospheric correction module.

In order to specify the products more precisely, we let  $R_d(\theta_0, \phi_0, \theta, \phi)$  denote the reflectance measured at the top of the atmosphere with the sun at zenith angle  $\theta_0$  and azimuth  $\phi_0$  and the satellite at  $(\theta, \phi)$ , and we let  $A_d(\theta_0)$  denote the corresponding albedo. The subscript  $d$  stands for ‘data’. We let lower case variables  $r_d(\theta_0, \phi_0, \theta, \phi)$  and  $\alpha_d(\theta_0)$  denote corresponding quantities measured at the surface. With these definitions, the indicatrix is

$$g_d(\theta_0, \phi_0, \theta, \phi) = r_d(\theta_0, \phi_0, \theta, \phi) / \alpha_d(\theta_0).$$

The purpose of the software is to estimate  $r_d$  and  $\alpha_d$ , not only for the sun-satellite geometry that pertained at the time of the observation, but also for a standard geometrical configuration with the sun at  $(\overline{\theta_0}, \overline{\phi_0})$  and satellite at  $(\overline{\theta}, \overline{\phi})$ , where the overbar indicates an arbitrary reference angle. These estimated quantities we denote by a circumflex; thus,  $\hat{r}_d$  and  $\hat{\alpha}_d$  are estimates of  $r_d$  and  $\alpha_d$  provided by MAPS.

In the course of obtaining the estimates, we will need, in addition to the optical properties of the atmosphere, a model for the surface BRDF and albedo, for which we use the notation  $r_m$  and  $\alpha_m$ , where the subscript  $m$  stands for ‘model’. The model indicatrix is then

$$g_m(\theta_0, \phi_0, \theta, \phi) = r_m(\theta_0, \phi_0, \theta, \phi) / \alpha_m(\theta_0).$$

As an illustration, Roujean’s model (Roujean et al., 1992) has

$$r_m = k_0 + k_1 f_1 + k_2 f_2,$$

where  $f_1$  and  $f_2$  are kernels representing geometric and volume scattering, and  $k_0$ ,  $k_1$  and  $k_2$  are numerical parameters. Both  $f_1$  and  $f_2$  depend only on the incident direction  $(\theta_0, \phi_0)$  and the exit direction  $(\theta, \phi)$ . For this model, the surface albedo is

$$\alpha_m = k_0 + k_1 I_1 + k_2 I_2,$$

where  $I_1$  and  $I_2$  are simple trigonometric functions that depend only on the solar zenith angle  $\theta_0$ . It is clear in this case that the indicatrix

$$g_m = \frac{k_0 + k_1 f_1 + k_2 f_2}{k_0 + k_1 I_1 + k_2 I_2}$$

depends only on the ratios  $k_1/k_0$  and  $k_2/k_0$ .

The algorithm and its various products are represented by the flow chart of figure 6. The circle labelled ATCO is the atmospheric correction algorithm developed by Mitchell and O’Brien (1993), the inputs to which are the reflectance  $R_d(\theta_0, \phi_0, \theta, \phi)$  at the top of the atmosphere and a model  $g_m(\theta_0, \phi_0, \theta, \phi)$  for the indicatrix. The output of ATCO is  $\hat{\alpha}_d(\theta_0)$ , the estimate of the surface albedo with the sun at zenith angle  $\theta_0$ . Subsequent steps shown in figure 6 lead to the products listed in table 1. Note that the first two products listed are obtained by replacing ATCO with a trivial UNIT algorithm whose output is equal to its input, thereby disabling all atmospheric correction.

*It must be stressed that only products 4, 5 and 6 have a sound physical basis, and therefore only these products should be used operationally. The other products are generated primarily as diagnostics.*

## 4.1 Module reflectance

Code supervising the generation of surface albedos (for both Lambertian and non-Lambertian surfaces), and reflectances (uncorrected or corrected for atmospheric effects and uncorrected or corrected to a reference geometry) is written in a single module, named reflectance. This module is accessed via three main calls: the first subroutine sets tables according to satellite number, the overpass date and time and the required output product; the second subroutine generates the required product (specified by the product number) given the reflectance factor, band, latitude and longitude of the surface element and sun illumination and satellite observation angles; the third subroutine releases memory allocated to tables set in the first.

Module reflectance uses two subsidiary modules: AtmosCorrection which supervises the process of applying atmospheric correction and generating surface albedo, and BRDFCorrection which supervises correction from a given geometry to a reference geometry. Most application programs would use module reflectance only. However, modules AtmosCorrection and BRDFCorrection could be used directly if required.

It should be clear from the above, that module reflectance and its two subsidiary modules are ‘stand-alone’ units that are independent of satellite data structures and formats and thus can be applied generally in a variety of contexts. All three modules are largely self documenting but require, in places, reference to Mitchell and O’Brien (1993), Roujean et al. (1992) and Staylor and Suttles (1986).

## 4.2 Module AtmosCorrection

Module AtmosCorrection contains all the code used in applying atmospheric correction. It is accessed via three primary subroutines: the first subroutine sets tables according to the mean aerosol optical depth over the scene and the satellite number; the second subroutine returns surface albedo for given values of reflectance factor, band, latitude and longitude of the surface element, sun and satellite view angles, aerosol optical depth, water column and  $g_m(\theta_0, \phi_0, \theta, \phi)$ ; the third subroutine releases memory allocated to tables set in the first.

The code essentially solves a modified form of equation 84 of Mitchell and O’Brien (1993) that allows aerosol optical depth and integrated water column to be specified as independent variables. In its original form these parameters had to be specified in advance, as they were used (explicitly in the case of aerosol optical depth and implicitly in the case of integrated water column) in the generation of underlying retrieval tables. Values of aerosol optical depth corresponding to the latitude and longitude of a given image element are interpolated from a grid of seasonal mean values derived from the Global

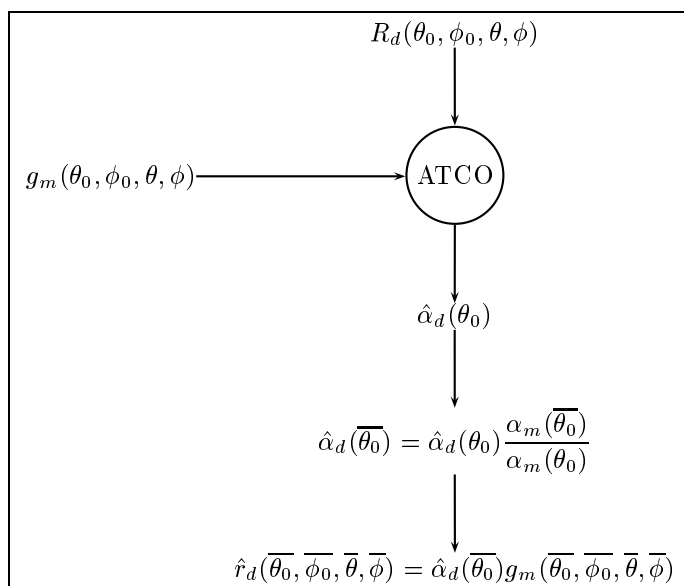


Figure 6: Flow chart for the atmospheric correction module.

Aerosol Data Set (GADS) as developed by Köpke et al. (1997). Values of water column for each surface element are interpolated from grid values generated twice daily by the DARLAM 18-level regional model (McGregor et al., 1993). Where DARLAM data are missing or unavailable, the code automatically extracts water column values from a grid of monthly mean values based on the NVAP data set (Randel et al., 1995). For both aerosol optical depth and water column, the user has the option of supplying a single value that is used for all elements of the image. In all cases, values for each element are supplied to AtmosCorrection — the setting of appropriate tables and the extraction of interpolated values is initiated from within module reflectance by separate modules that manage access to aerosol optical depth and water column data respectively.

AtmosCorrection has been tested thoroughly. Reflectance factors as sensed by bands 1 and 2 of the AVHRR instrument were calculated using DARSOS (code that implements the radiative transfer algorithm described in the appendix to Mitchell et al. (1996)) for eleven values of albedo, eleven values of aerosol optical depth and nine sun-satellite configurations. An early version of the module was used to retrieve albedo with water column fixed at the value used in generating the reflectance factors. Errors in retrieved albedos were generally small and of the same order as errors obtained using the unmodified algorithm where comparable. Errors were particularly small for cases where aerosol optical depth approached the aerosol optical depth assumed in the generation of the underlying retrieval tables — here 0.125.

In order to address speculation that the 6S code of Vermote et al. (1997) would prove more satisfactory than the then current version of the AtmosCorrection code, the test reported above was repeated with 6S code substituted for the AtmosCorrection code. Results were similar in all respects but the 6S code ran more slowly — so much so that it could not be considered a viable option for pixel-by-pixel processing. Table 2 shows comparative performance figures. The superior performance of the code employed here is attributed to the fact the algorithm on which it is based was formulated to make extensive use of pre-compiled, retrieval tables.

Band	Aerosol optical depth	Atmos Correction (s pixel <sup>-1</sup> )	6S (s pixel <sup>-1</sup> )	ratio
1	=0	.000160	5.3	33,000
1	>0	.000160	96.6	604,000
2	=0	.000154	3.1	20,000
2	>0	.000154	55.5	360,000

Table 2: Relative speeds of 6s code and AtmosCorrection code.

Where the early version of AtmosCorrection used one set of underlying retrieval tables, the present module uses thirty two sets: one for each of the four optical depths 0.05, 0.15, 0.25 and 0.35 and, for each of these, eight values of integrated water column, 0, 10, 20, 30, 40, 50, 60 and 70 kg m<sup>-2</sup>. The algorithm selects the optical depth closest to the mean optical depth for the scene to be analysed and reads into memory all eight sets of retrieval tables corresponding to this optical depth. The module then uses interpolation between consecutive water column tables to perform a retrieval for a given water column value.

This latest version of the module was tested, as was the earlier version, with calculated values of reflectance factors and nine sun-satellite configurations. However, in this instance, the test used one value of surface albedo (0.25), three values of optical depth and three values of integrated water column. Errors in retrieved albedos were small, being less than about 3% for approximately 90% of cases and never greater than 7%.

### 4.3 Module BRDFCorrection

Module BRDFCorrection contains all code associated with BRDF correction. It is accessed via three primary subroutines and two functions: the first subroutine sets tables of BRDF coefficients according to the overpass date and a user-selected BRDF model name (see below); the second subroutine retrieves from these tables BRDF coefficients corresponding to the latitude and longitude of an image element and a satellite band; the third subroutine releases memory allocated to tables set in the first; the first

function returns  $r_m(\theta_0, \phi_0, \theta, \phi)$  for a given sun-satellite geometry (actual or reference geometry and using either the Roujean (Roujean et al., 1992) or Staylor and Suttles (Staylor and Suttles, 1986) algorithm); the second function returns  $\alpha_m(\theta_0)$  for a given sun zenith angle (again, actual or reference geometry and either the Roujean or Staylor and Suttles algorithm). Note that the code is very general and any number of BRDF models may be added to the list of options with very little effort. Furthermore, specification of the model to be used is effected through a flexible metadata structure that allows the user full control without needing to modify (or even examine) the code.

A metadata file is provided for Roujean’s BRDF model (Roujean et al., 1992) for the Australian continent and also for specific sites using the BRDF model proposed by Staylor and Suttles (1986). Parameters for the former are derived from POLDER data acquired during the ten-month life of ADEOS, while those for the latter are obtained from time series of AVHRR data as outlined by O’Brien et al. (1998). The BRDF data for the specific sites is intended for R&D rather than operational use. As more data for the indicatrix become available from new sensors, such as MODIS, MISR and POLDER on ADEOS II, corresponding metadata will be added to the database. Options for analysis of retrospective data are more limited, but include using the indicatrix derived from POLDER data or the historical AVHRR archive, again using the algorithm developed by O’Brien et al. (1998).

The two operational models currently available are:

- (i) `POLDER_Roujean_Month`. This model employs the Roujean BRDF model with coefficients derived using POLDER data for Australia extracted from the POLDER level 3 product ‘Surface Directional Signature’. Coefficients correspond to monthly values irrespective of year. They are available on an approximately 6km grid. Here we take the nearest valid datum to the image element being processed.
- (ii) `POLDER_Roujean_YearMonth`. This model employs the Roujean BRDF model with coefficients derived using POLDER data for Australia. Coefficients correspond to monthly values for specific years. Grid spacing and selection are as for (i).

There are six site-specific R&D models available. They are:

- (i) `AVHRR_Staylor_Suttles_Tinga_Tingana_Day`. This model uses the Staylor and Suttles BRDF model with coefficients derived using AVHRR data for Tinga Tingana (O’Brien et al., 1998). Coefficients correspond to specific days and strictly speaking apply to the Tinga Tingana (139.833E, -29.000N) site exclusively.
- (ii) `AVHRR_Staylor_Suttles_Tinga_Tingana_Month`. This model uses the Staylor and Suttles BRDF model with coefficients derived using AVHRR data for Tinga Tingana. Coefficients correspond to monthly values irrespective of year and, strictly speaking, apply to the Tinga Tingana site exclusively.
- (iii) `AVHRR_Staylor_Suttles_Tinga_Tingana_YearMonth`. This model uses the Staylor and Suttles BRDF model with coefficients derived using AVHRR data for Tinga Tingana. Coefficients correspond to monthly mean values for specific years and, strictly speaking, apply to the Tinga Tingana site exclusively.
- (iv) `AVHRR_Staylor_Suttles_Hay_Day`. As for (i) but derived using data for Hay (145.305E, -34.392N).
- (v) `AVHRR_Staylor_Suttles_Hay_Month`. As for (ii) but derived using data for Hay.
- (vi) `AVHRR_Staylor_Suttles_Hay_YearMonth`. As for (iii) but derived using data for Hay.

An obvious extension of the present work is to expand the site-specific AVHRR models to a single operational model giving continental coverage for the historical time series. A simple and straightforward plan to accomplish this using archived AVHRR data has been formulated. It awaits funding for implementation.

#### 4.4 Test/demonstration code and data

All modules described under this section are supplied as products of the present project.

In addition we make available a test and demonstration program named Reflectance2000 that takes raw AVHRR data written in DISIMP format and generates six, or optionally, ten output channels as follows:

```
channel 1  uncorrected reflectance for band 1 * 100 (Refl1)
channel 2  uncorrected reflectance for band 2 * 100 (Refl2)
channel 3  NDVI based on reflectance factors * 1000 (NDVIRF)
channel 4  reflectance product for band 1 * 100 (Refp1)
channel 5  reflectance product for band 2 * 100 (Refp2)
channel 6  NDVI based on reflectance product * 1000 (NDVIRp)
```

and optionally,

```
channel 7  satellite azimuth (degrees) * 10 (SatAz)
channel 8  satellite elevation (degrees) * 10 (SatEl)
channel 9  sun azimuth (degrees) * 10 (SunAz)
channel 10 sun elevation (degrees) * 10 (SunEl)
```

where p is the specified product number (1 – 6).

The process requires the generation of reflectance factors, geographic location and sun illumination and satellite viewing angles. Reflectance factors are generated as for Cloud2000 (see section 3.2) using the CalWatch data set and module AVHRRVisCal. Geographic location and sun and satellite angles are generated using the MAPS navigation modules.

The procedure employed here to achieve accurate navigation is best described with reference to figure 1. Program SATLOC (Dilley and Elsum, 1994) locates features with known geographic co-ordinates in image data and infers departures in satellite location from the Brouwer-Lyddane (Lyddane, 1963) model embodied in module NOAAOrbit and departures in the AVHRR instrument package yaw from an assumed value of zero. It writes to the DISIMP file header parameters that quantify these offsets in terms of image line number. In all subsequent navigation, accurate satellite location and yaw is calculated by correcting model location and yaw using the line number and parameters recorded in the file header.

Reflectance2000 employs the MAPS calibration and navigation modules to generate the calibrated, navigated data required by module reflectance. It should be emphasized, however, that module reflectance is indeed modular and that it will operate independently of the MAPS calibration and navigation modules. In fact it requires only inputs that define some overall conditions such as satellite number, date and time of overpass and required reflectance product and then, for each element, reflectance factor, band number, latitude and longitude, sun and satellite zenith angles and sun-satellite difference in azimuth.

Reflectance2000 was used to generate the images shown in figures 2 and 3. This series of images demonstrates the effectiveness of the correction procedures described above. Using AVHRR data derived from two successive satellite overpasses with very different sun-satellite geometries, the discontinuity in intensity evident at the mid-point of the overlap region for uncorrected reflectances is removed when these same reflectances are corrected for atmospheric effects and to a standard illumination and observation geometry. All data files, remapping and splicing programs required to reproduce this series of images have been included in the MAPS package.

#### 4.5 Sensitivity analysis

The effect on reflectances (and hence on NDVI) of corrections made using the present models depends on numerous factors and any attempt to quantify these effects would need to take all factors into account. Here we simply illustrate the effects using a representative image of south-eastern Australia (NOAA-14, afternoon ascending overpass of 10 December 1997, orbit number 15177). We processed the image using Reflectance2000 under three sets of conditions: no aerosol and no water vapour (Rayleigh); no aerosol and a water column of  $30 \text{ kg m}^{-2}$ ; no water vapour and an aerosol optical depth of 0.10. We extracted reflectances from the image for nine sites that encompassed a range of reflectance signatures.

The results are plotted in figure 7. We make the following observations:

- correction for a purely Raleigh atmosphere is associated with a decreases in band 1 reflectance at all sites — the effect on band 2 reflectances varies from site to site with some evidence of

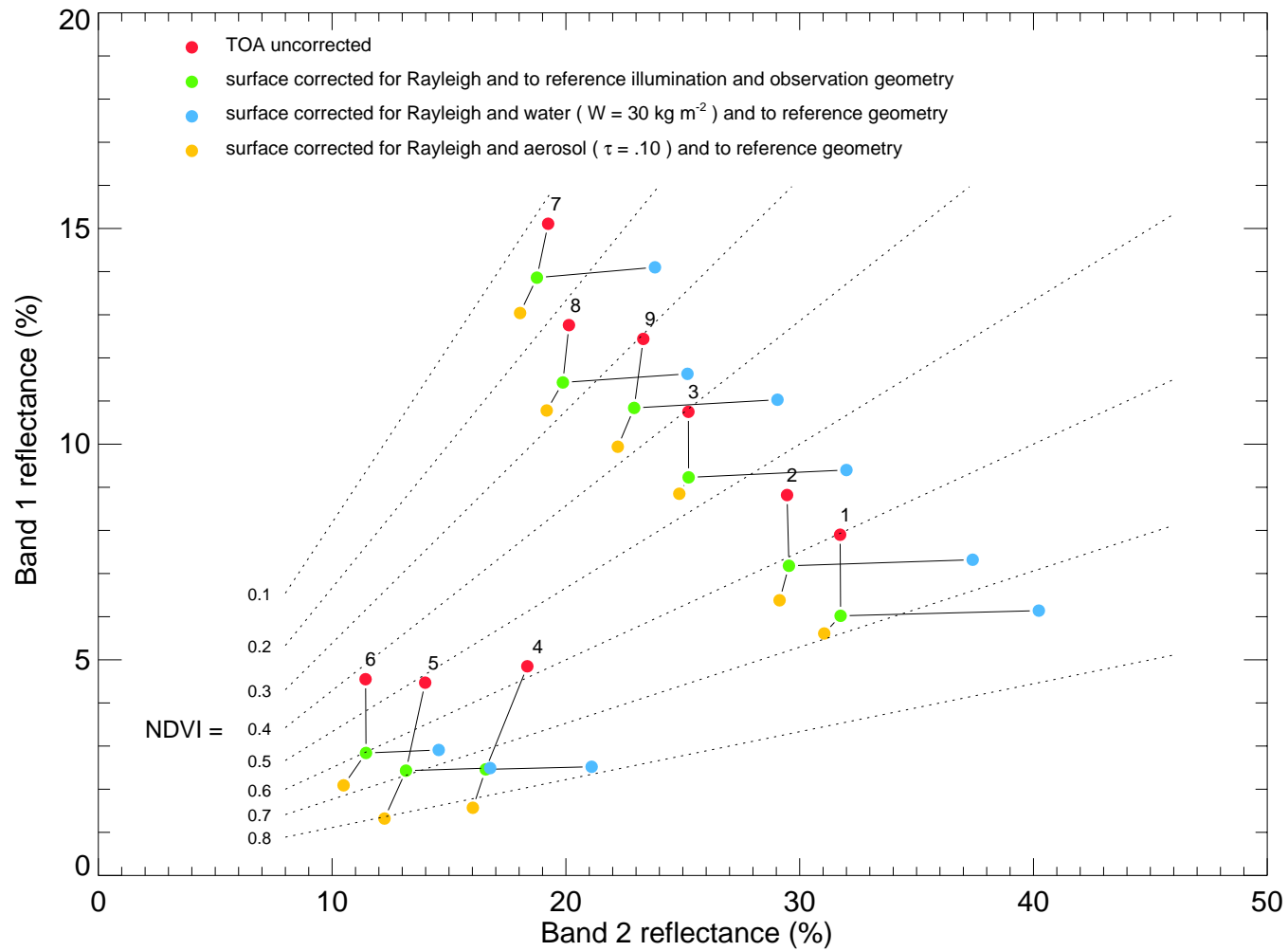


Figure 7: Uncorrected top of the atmosphere reflectances and variously corrected surface reflectances extracted for nine sites located in an image of south-eastern Australia. The image data derive from an afternoon ascending overpass of NOAA-14 for 10/12/1997, orbit number 15177.

increases at higher levels of reflectance and decreases at lower levels;

- correction for water vapour is associated with relatively large increases in band 2 reflectances at all sites compared to changes in band 1 reflectances;
- correction for water vapour is associated with increases in NDVI at all sites with the effect being more pronounced at lower values of NDVI than at higher values;
- correction for aerosol loading is associated with decreases in both band 1 and band 2 reflectances at all sites with the magnitude of the response in band 1 generally exceeding that in band 2;
- correction for aerosol loading is associated with increases in NDVI at all sites with the effect being more pronounced at higher values of NDVI than at lower values.
- corrections for a Rayleigh atmosphere, water vapour and aerosol loading under commonly encountered conditions are associated with relatively large changes in reflectances and NDVI values — failure to make these corrections would normally introduce substantial error.

The non-linear nature of the effect of corrections on NDVI noted above is also evident when one compares the middle and bottom images of figure 4.

## 5 Software packaging

The MAPS package is distributed as a compressed tar file, MAPS.tar.Z, and a Read.me file that covers installation, testing and running the demonstration programs on supplied data. The Read.me document is reproduced here as Appendix A.

## 6 Conclusion

The MAPS package offers exciting prospects for analysis (and re-analysis) of AVHRR data. In generating products that are independent of sensor sensitivity and location, sun illumination and the vagaries of an intervening atmosphere — products that truly represent physical properties of the surface — the code opens up possibilities for improved performance in a number of traditional remote sensing endeavours. Examples that come readily to mind are improved fire scar detection and mapping (where the scar is identified in terms of its surface reflectance relative to the surface reflectance of its surroundings), improved cloud detection and mapping (where the cloud is identified by its reflectance relative to a historically determined, mean surface reflectance of the image element) and improved vegetation greenness and vegetation moisture determination — and hence improved GCI maps (via an NDVI based on surface reflectances rather than the traditionally employed top of atmosphere reflectances).

## 7 Acknowledgements

The authors acknowledge with gratitude the assistance of John McGregor and Jack Katzfey who set in place code to generate and deliver, in a suitable format, water column output from the DARLAM model, and the assistance of Clive Ellum who facilitated the secure delivery of these data across the CAR network.

The POLDER data were supplied courtesy of CNES.

## References

- Dilley, A. C., and M. Edwards, 1998a: The automatic processing of ASDA format NOAA HRPT data at CSIRO DAR. Technical report, CSIRO Division of Atmospheric Research, Aspendale, Victoria, Australia. Internal Paper No. 6, 41 pp.
- Dilley, A. C., and M. Edwards, 1998b: Satellite-based monitoring of grassland curing in Victoria, Australia. *The Globe, J. of The Australian Map Circle Inc.*, **47**.
- Dilley, A. C., and C. E. Ellum, 1994: Improved AVHRR data navigation using automated land feature recognition to correct a satellite orbital model. Technical report, CSIRO Division of Atmospheric Research, Aspendale, Victoria, Australia. Technical Paper No. 34, 22 pp.

- Köpke, P., M. Hess, I. Schult, and E. P. Shettle, 1997: Global aerosol data set. Technical report, Max-Planck-Institut für Meteorologie. Report No. 243.
- Lyddane, R. H., 1963: Small eccentricities or inclinations in the Brouwer theory of the artificial satellite. *The Astronomical J.*, **68**, 555–558.
- McGregor, J. L., K. J. Walsh, and J. J. Katzfey, 1993: Nested modelling for regional climate studies. *Modelling Change in Environmental Systems*, A. J. Jakeman, M. B. Beck, and M. J. McAleer, Eds., Wiley, 367–386.
- Mitchell, R. M., 1997: CalWatch: Calibration status of the NOAA AVHRR solar reflectance channels. CSIRO Atmospheric Research, website <http://www.dar.csiro.au/rs/calwatch.htm>.
- Mitchell, R. M., 1999: Calibration status of the NOAA AVHRR solar reflectance channels: CalWatch Revision 1. Technical report, CSIRO Atmospheric Research, Aspendale, Victoria, Australia. Technical Paper No. 42, 20 pp.
- Mitchell, R. M., and D. M. O'Brien, 1993: Correction of AVHRR shortwave channels for the effects of atmospheric scattering and absorption. *Remote Sens. Environ.*, **46**, 129–145.
- Mitchell, R. M., D. M. O'Brien, and B. W. Forgan, 1992: Calibration of the NOAA AVHRR shortwave channels using split pass imagery: I. Pilot study. *Remote Sens. Environ.*, **40**, 57–65.
- Mitchell, R. M., D. M. O'Brien, and B. W. Forgan, 1996: Calibration of the AVHRR shortwave channels: II Application to NOAA 11 during early 1991. *Remote Sens. Environ.*, **55**, 139–152.
- O'Brien, D. M., R. M. Mitchell, M. Edwards, and C. C. Elsum, 1998: Estimation of BRDF from AVHRR short-wave channels: tests over semiarid Australian sites. *Remote Sens. Environ.*, **66**, 71–86.
- Randel, D. L., T. H. V. Harr, M. A. Ringerud, D. L. Reinke, G. L. Stephens, C. L. Combs, T. J. Greenwald, and I. L. Wittmeyer, 1995: An introduction to the NASA Water Vapour Project Data Set (NVAP). Technical report, National Aeronautics and Space Administration, Washington, D. C., USA. Under Contract NASW-4715.
- Rao, C. R. N., and J. Chen, 1995: Inter-satellite calibration linkages for the visible and near infrared channels of the Advanced Very High Resolution Radiometer on NOAA-7, -9, and -11 spacecraft. *Int. J. Remote Sens.*, **16**, 1931–1942.
- Rao, C. R. N., and J. Chen, 1996: Post-launch calibration of the visible and near-infrared channels of the Advanced Very High Resolution Radiometer on the NOAA-14 spacecraft. *Int. J. Remote Sens.*, **17**, 2743–2747.
- Roujean, J., M. Leroy, and P. Y. Deschamps, 1992: A bidirectional reflectance model of the earth's surface for correction of remote sensing data. *J. Geophys. Res.*, **97**, 20,455–20,468.
- Staylor, W. F., and J. T. Suttles, 1986: Reflection and emission models for deserts derived from Nimbus 7 ERB scanner measurements. *J. Clim. Appl. Meteorol.*, **25**, 196–202.
- Turner, P. J., H. L. Davies, P. C. Tildesley, and C. Rathbone, 1998: Common AVHRR Processing Software (CAPS). *Proceedings of the Land AVHRR Workshop - 9th Australian Remote Sensing and Photogrammetry Conference, Sydney July 1998.*, T. R. McVicar, Ed. CSIRO Land and Water, Canberra, ACT, 51–58.
- Vermote, E. F., D. Tanré, J. L. Deuzé, M. Herman, and J. J. Moncrette, 1997: Second simulation of the satellite signal in the solar spectrum (6S): an overview. *IEEE Trans. Geosci. Remote Sens.*, **35**, 675–686.

## Appendix A

### Read.me document supplied with Version 1.0 release

#### MODULAR AVHRR PROCESSING SOFTWARE (MAPS)

##### INTRODUCTION

The accompanying MAPS.tar.Z file contains code developed under the Earth Observation Centre Project: "Operational AVHRR processing modules: atmospheric correction, cloud masking and BRDF compensation" (O'Brien et al 1998a, Dilley et al 1999, Dilley et al 2000). This release contains modules for integrated atmospheric correction and BRDF compensation, and cloud masking.

The file also contains:

- . test programs that can be used to ensure correct installation of code and data;
- . programs that demonstrate the application of the modules in processing AVHRR image data;
- . supporting modules that calibrate and navigate the data (required by the test and demonstration programs but not the modules for atmospheric correction and BRDF compensation and cloud masking);
- . modules that provide low-level functionality;
- . libraries that provide data access and management functions (required by the test and demonstration programs but not the modules for atmospheric correction and BRDF compensation and cloud masking);
- . test images and reference output data
- . data tables required for atmospheric correction;
- . data tables required for thermal sensor calibration;
- . a climatological record of aerosol optical depth based on the GADS data set (Kopke et al, 1997);
- . a climatological record of water column based on the NVAP data set (Randel et al, 1997);
- . a limited (9-month) daily record of water column based on the 18-level regional forecast model DARLAM (McGregor et al 1993);
- . a 'make' file to build modules, libraries and programs;
- . a list of required environmental variables.

The atmospheric correction and BRDF compensation modules operate under the control of a supervising module named reflectance. This module generates several products ranging from uncorrected, top-of-the-atmosphere reflectances to surface reflectances corrected for atmospheric effects and corrected to a standard illumination and viewing geometry.

The atmospheric correction module, AtmosCorrection, is based on an algorithm developed by Mitchell and O'Brien (1993) and subsequently modified by Dilley (paper in preparation). The modified algorithm allows aerosol optical depth and integrated water column to be specified as independent variables that may vary on a pixel by pixel basis. Values for aerosol optical depth and integrated water column are obtained from observed values or data bases of contemporary analysed fields or, in the absence of these, climatological average values. In the case of aerosol optical depth, climatological values are obtained from the GADS data set

(Kopke et al, 1997). In the case of water vapour, contemporary data is derived from the DARLAM regional model (McGregor et al, 1993) while climatological average values are obtained from the NVAP data set (Randel et al, 1995). It is anticipated that access to contemporary DARLAM data will be provided as the need arises.

The BRDF compensation module, BRDFCorrection, implements correction from a given illumination and observation geometry to a standard reference geometry. It supports eight BRDF models including those described by O'Brien et al (1998b), Staylor and Suttles (1986) and Roujean et al (1992).

The cloud masking module implements an algorithm first described in Dilley and Edwards (1998). The algorithm operates using the AVHRR parameters of band 1 reflectance factor, variance of band 1 reflectance factor, a simple function of the ratio of band 1 to band 2 reflectance factor and brightness temperature derived from band 4. The value of each parameter is examined in relation to three pre-set threshold values for that parameter. Passing the first threshold test scores a point in favour of cloud, passing the second threshold test earns a bonus point (cloud very likely) and passing the third threshold test earns a demerit point (cloud very unlikely). After all four parameters are tested, the cloud mask is set if the point score totals 2 or more.

The MAPS code was developed and tested by Mac Dilley and Mary Edwards (e-mail: Mac.Dilley@dar.csiro.au, Mary.Edwards@dar.csiro.au). The authors give notice that they will not be responsible for consequences flowing from any unauthorised changes to the code, no matter how minor or trivial those changes may seem.

The code was developed on Sun UNIX workstations running under Solaris 2.5. It was written in Fortran 90 and compiled using Sun Workshop Compiler Fortran 90 2.0. All code was written to the Fortran 90 standard and should compile under any standard-compliant compiler. The Sun Workshop Compiler provided links to the libraries used here for data access and management and compiled under Fortran 77. Any alternative compiler would need to provide the same functionality if it is to build the test and demonstration programs supplied here.

## INSTALLATION

1. Place MAPS.tar.Z in suitable directory (the MAPS directory).
2. uncompress MAPS.tar.Z
3. tar xvf MAPS.tar .

src/mains should contain the source code of demonstration programs Reflectance2000, Cloud2000 and Splice.

src/test should contain the source code of test programs TestAVHRRVisCal and MAPSTest

src/modules should contain the source code of the supervisory module, reflectance, the atmospheric correction module, AtmosCorrection, the BRDF compensation module, BRDFCorrection and the cloud mask module,

CloudMask. It should also contain the source code of additional modules required to test and demonstrate these primary modules.

include should contain several 'include' files that give access to data stored in common blocks defined in the data access and management libraries.

etc should now contain Makefile which is used to build libraries and binaries.

lib should contain the libraries that provide data access and management functions - cdi9.a, dblock.o, disimp.a, vista.a.

data/atmos should contain all the data tables required for atmospheric correction

data/disimp should contain various test input and reference output image data.

data/cal should contain tables of data required for AVHRR thermal calibration and brightness temperature generation.

data/specs should contain the cloud masking specification file, CloudMask.spec and the reflectance specification file reflectance.spec.

4. cd etc
5. edit MAPSEnvVariables to relate full path name of your chosen MAPS directory to environmental variable MAPSPath and the appropriate pathname for your CalWatch directory to environmental variable AVHRRVisCalPath.
6. source MAPSEnvVariables  
(or, alternatively, copy into .cshrc file and source .cshrc)
7. make
8. source ~/.cshrc

lib should now also contain the module library ModLib.a and associated .mod files.

bin should now contain the binaries of the test and demonstration programs: TestAVHRRVisCal, MAPSTest, Reflectance2000, Cloud2000 and Splice.

#### TESTING

1. Run TestAVHRRVisCal supplying responses consistent with the worked examples provided in Mitchell (1999). Check that output agrees with Mitchell results. (Our tests show a discrepancy with Mitchell results for the case C2 = 167. We get I2 = 65.8961 cf Mitchell I2 = 66.0. The difference is due to a rounding error in Mitchell)
2. cd \$MAPSPath/data/disimp

Then run MAPSTest - just enter MAPSTest at the command line. This test program reads the DISIMP-formatted AVHRR raw-data image file MAPSTest.dat and generates the DISIMP-formatted output file MAPSTest.out. The latter contains a 10-pixel x 10-line image with 10 channels:

```
channel 1    reflectance factor for band 1 * 100  (ReflF1)
channel 2    reflectance factor for band 2 * 100  (ReflF2)
channel 3    brightness temperature for band 4 * 100 (BTemp4)
channel 4    brightness temperature for band 5 * 100 (BTemp5)
channel 5    satellite azimuth * 10      (SatAz)
channel 6    satellite elevation * 10     (SatEl)
channel 7    sun azimuth * 10            (SunAz)
channel 8    sun elevation * 10          (SunEl)
channel 9    surface albedo for band 1 * 100 (SurfA1)
channel 10   surface albedo for band 2 * 100 (SurfA2)
```

Satisfactory operation of the atmospheric correction module should be checked by comparing the values in all channels with the values in the reference image MAPSTest.ref. The DISIMP utility dmping provides a convenient means of displaying values in the output and reference images.

Note: MAPSTest will not overwrite an existing output file. Hence MAPSTest.out should be removed before MAPSTest is repeated.

### 3. Reflectance2000 TestRefl2000.spec MapsTest.dat

This test reads the DISIMP-formatted AVHRR raw-data image file MAPSTest.dat and generates the DISIMP-formatted output file MAPSTest.rfl. The latter contains a 10-pixel x 10-line image with 6 channels:

```
channel 1    uncorrected reflectance for band 1 * 100  (Refl11)
channel 2    uncorrected reflectance for band 2 * 100  (Refl12)
channel 3    NDVI based on reflectance factors * 1000 (NDVIRF)
channel 4    reflectance product for band 1 * 100  (Reflp1)
channel 5    reflectance product for band 2 * 100  (Reflp2)
channel 6    NDVI based on reflectance product * 1000 (NDVIRp)
```

where p is the specified product number - here = 6.

MAPSTest.rfl should be identical to the supplied reference file MAPSTestRefl.ref. The DISIMP utility dmping provides a convenient means of displaying values in the output and reference images.

## DEMONSTRATION

1. cd \$MAPSPath/data/disimp

2a. Reflectance2000 Reflectance2000.spec n14\_11367.dat  
Reflectance2000 Reflectance2000.spec n14\_11368.dat

This runs program Reflectance2000 on the DISIMP-formatted AVHRR raw-data image files n14\_11367.dat and n14\_11368.dat with options as specified in reflectance.spec to produce the

DISIMP-formatted output files n14\_11367.rfl and n14\_11368.rfl  
The latter contain images of eastern and western Australia  
respectively with channels as per TEST (3) above.

b. noawrp\_do

and respond to prompts as follows:

```
Enter name of input image
Name of file? n14_11367.rfl
Enter up to 6 input channels [1-6](1-6): [return] (default)
lat & long of northwest corner -10.0, 110.0
lat & long of southeast corner -45.0, 155.0
Enter the no of grid points: lat, lng (11,11) 15, 15
Enter output increments (lat, lng) .0685, .0763
Output image file
Name of file? n14_11367.wrp
Enter output image description [124 Chs.]
: [return] (default)
Interpolation method .....: [return] (default)
```

This procedure should produce an output file n14\_11367.wrp that  
contains the data of the input file, n14\_11367.dat, remapped to  
co-ordinates that are rectilinear in latitude and longitude.

c. noawrp\_do

and repeat b above for n14\_11368.rfl.

d. Splice

and respond to prompts as follows:

```
Input image (left)
Name of file? n14_11368.wrp
Input image (right)
Name of file? n14_11367.wrp
Output image
Name of file? n14_11368_7p6.spl
Enter output image description [124 Chs.]
: NOAA-14 11368 11367 15/03/97
Enter overlap type: 3
```

This should produce an output image file that is identical with the  
supplied file n14\_11368\_7p6\_DEMO.spl and, when displayed, should  
produce images for channels 2 and 6 that are identical to the images  
shown in figure 2 of the EOC Project Final Report (Dilley et al, 2000).  
The IDL program DISPLAY (Dilley, 1996) provides a straightforward  
means of displaying images written in DISIMP format.

The specification file data/specs/reflectance.spec may be edited  
at run-time to explore the effects of changing options such as the  
product number (to produce the images in figure 2 of the EOC Project  
Final Report) and values of aerosol optical depth and integrated water  
column. Note, however, that Reflectance2000 will not overwrite an  
existing output file. Hence any existing output file should be  
removed before the program is re-run.

3. Cloud2000 Cloud2000.spec n14\_21527\_VIC.dat

This runs demonstration program Cloud2000 on the DISIMP-formatted

AVHRR raw-data image file n14\_21527\_VIC.dat with options as specified in Cloud.spec. Cloud generates the DISIMP-formatted output image file n14\_21527\_VIC.cld. The latter contains an image of eastern Victoria with 6 channels:

```
channel 1    reflectance factor for band 1 * 100 (ReflF1)
channel 2    reflectance factor for band 2 * 100 (ReflF2)
channel 3    brightness temperature for band 4 * 100 (BTemp4)
channel 4    variance of reflectance factor for band 1 * 100 (VarnR1)
channel 5    ABS( A - ( ReflF1 ) / ( ReflF2 ) ) * 100 (RaR1R2)
channel 6    cloud mask ( 0, 1 ) (CldMsk)
```

The output image file should be identical to the supplied file n14\_21527\_VIC\_DEMO.cld and, when displayed, should produce a cloud mask identical to that shown in figure 4 of the EOC Project Final Report. The IDL utility DISPLAY is convenient for this purpose and is also convenient for quickly assessing the effects of each threshold parameter in shaping the generated cloud mask.

The specification file data/specs/CloudMask.spec may be edited at run-time to explore the effects of changing parameter threshold values. Note, however, that Cloud2000 will not overwrite an existing output file. Hence any existing output file should be removed before the program is re-run.

#### REFERENCES

- Dilley, A. C., 1996: Interactive display of images written in DISIMP file format using the IDL program DISPLAY. CSIRO Division of Atmospheric Research Internal Paper No. 1. 55pp.
- Dilley A. C. and M. Edwards, 1998: The automatic processing of ASDA format NOAA HRPT data at CSIRO DAR. CSIRO Division of Atmospheric Research Internal Paper No. 6. 41pp.
- Dilley, A. C., M. Edwards, D. M. O'Brien and R. M. Mitchell, 1999: Operational AVHRR processing modules: atmospheric correction, cloud masking and BRDF compensation. EOC Project Interim Report.
- Dilley, A. C., M. Edwards, D. M. O'Brien and R. M. Mitchell, 2000: Operational AVHRR processing modules: atmospheric correction, cloud masking and BRDF compensation. EOC Project Final Report.
- Kopke, P., M. Hess, I. Schult, and E. P. Schettle, 1997: Global aerosol data set. Technical report, Max-Planck-Institut fur Meteorologie. Report No. 243.
- McGregor, J. L., K. J. Walsh and J. J. Katzfey, 1993: Nested modelling for regional climate studies. Modelling Change in Environmental Systems, A. J. Jakeman, M. B. Beck and M. J. McAleer, Eds., Wiley, 367-386.
- Mitchell, R. M. and D. M. O'Brien, 1993: Correction of AVHRR shortwave channels for the effects of atmospheric scattering and absorption. Remote Sens Environ., 46, 129-145.
- Mitchell, R. M., 1999: Calibration status of the NOAA AVHRR solar

- reflectance channels: CalWatch Revision 1. Technical report, CSIRO Atmospheric Research, Aspendale, Victoria, Australia. Technical Paper No. 42, 20pp.
- O'Brien, D. M., R. M. Mitchell, A. C. Dilley and M. Edwards, 1998a: Operational AVHRR processing modules: atmospheric correction, cloud masking and BRDF compensation. EOC Project Proposal.
- O'Brien, D. M., R. M. Mitchell, M. Edwards and C. C. Elsum, 1998b: Estimation of BRDF from AVHRR short-wave channels: tests over semiarid Australian sites. *Remote Sens. Environ.*, 66, 71-86.
- Staylor, W. F., and J. T. Suttles, 1986: Reflection and emission models for deserts derived from Nimbus ERB scanner measurements. *J. Clim. Appl. Meteorol.*, 25, 196-202.
- Randel, D. L., T. H. Vonder Harr, M. A. Ringerud, D. L. Reinke, G. L. Stephens, C. L. Combs, T. J. Greenwald, I. L. Wittmeyer, 1995: An introduction to the NASA Water Vapour Project Data Set (NVAP). Technical report, National Aeronautics and Space Administration, Washington, D. C. USA. Under Contract NASW-4715.
- Roujean, J-L., M. LeRoy, and P. Y. Deschamps, 1992: A bidirectional reflectance model of the earth's surface for correction of remote sensing data. *J. Geophys. Res.*, 97, 20,455-20,468.